Available online at www.sciencedirect.com
SCIENCE DIRECT
Biochemical and Biophysical Research Communications 347 (2006) 133–140
BBRC
www.elsevier.com/locate/ybbrc

Paramagnetic particles carried by cell-penetrating peptide tracking of bone marrow mesenchymal stem cells, a research in vitro ☆

Min Liu [a], You-min Guo [a,*], Qi-fei Wu [b], Jun-le Yang [a], Peng Wang [a], Si-cen Wang [c], Xiao-juan Guo [a], Yong-Qian Qiang [a], Xiao-Yi Duan [a]

[a] *Imaging Center, The 2nd Affliated Hospital of Medical School, Xi'An Jiao Tong University, Xi'An City ShaanXi Province 710004, China*
[b] *Cancer Research Center, Key Laboratory of Environment and Genes Related to Diseases of Ministry of Education, Xi'an Jiaotong University, Xi'An City ShaanXi Province 710061, China*
[c] *The Department of Pharmacy, Medical School, Xi'An Jiao Tong University, Xi'An City ShaanXi Province 710061, China*

Received 4 June 2006
Available online 22 June 2006

Abstract

The ability to track the distribution and differentiation of stem cells by high-resolution imaging techniques would have significant clinical and research implications. In this study, a model cell-penetrating peptide was used to carry gadolinium particles for magnetic resonance imaging of the mesenchymal stem cells. The mesenchymal stem cells were isolated from rat bone marrow by Percoll and identified by osteogenic differentiation in vitro. The cell-penetrating peptides labeled with fluorescein-5-isothiocyanate and gadolinium were synthesized by a solid-phase peptide synthesis method and the relaxivity of cell-penetrating peptide-gadolinium paramagnetic conjugate on 400 MHz nuclear magnetic resonance was $5.7311 \pm 0.0122\ \mathrm{mmol}^{-1}\ \mathrm{s}^{-1}$, higher than that of diethylenetriamine pentaacetic acid gadolinium ($p < 0.05$). Fluorescein imaging confirmed that this new peptide could internalize into the cytoplasm and nucleus. Gadolinium was efficiently internalized into mesenchymal stem cells by the peptide in a time- or concentration-dependent fashion, resulting in intercellular T1 relaxation enhancement, which was obviously detected by 1.5 T magnetic resonance imaging. Cytotoxicity assay and flow cytometric analysis showed the intercellular contrast medium incorporation did not affect cell viability and membrane potential gradient. The research in vitro suggests that the newly constructed peptides could be a vector for tracking mesenchymal stem cells.

Keywords: Mesenchymal stem cells; Cell-penetrating peptide; Gadolinium; Fluorescein; Magnetic resonance imaging

Mesenchymal stem cells are multipotent progenitors capable of differentiation into various types of connective tissues. Numerous studies [1–4] confirm relatively wide differentiation potential of these cells. They can be induced in vitro to osteogenic, adipogenic, and chondrogenic differentiation. In addition, they differentiate into tenocytes, hematopoietic stroma, skeletal, and smooth muscle tissue, myocardial tissue, as well as astrocytes, oligodendrocytes, neurons, etc. The ability to track the distribution and differentiation of progenitor and stem cells by high-resolution in vivo imaging techniques would have significant clinical and research implications. Developments in MR imaging have enabled in vivo imaging at/near microscopic resolution. In order to visualize and track stem and progenitor cells by magnetic resonance imaging, it is necessary to tag cells magnetically. Although contrast agents using paramagnetic metals such as gadolinium are routinely used in magnetic resonance imaging to shorten longitudinal relaxation times of water protons, they are confined to extracellular spaces. Cell-penetrating peptides (CPPs) have recently been used as an efficient way of internalizing a number of cargos into cells [5].

☆ This work is supported by the Doctoral Foundation of Xi'An Jiao Tong University (dfxjtu2005-09).
* Corresponding author.
E-mail addresses: mikie0763@126.com, cjr.guoyoumin@vip.163.com (Y. Guo).

0006-291X/$ - see front matter © 2006 Elsevier Inc. All rights reserved.
doi:10.1016/j.bbrc.2006.06.081

We hypothesized that a model peptide-based CPPs could carry gadolinium by diethylenetriaminepentaacetic acid (DTPA) internalizing into stem cells for tracking.

Materials and methods

Peptide synthesis. A L-CPP, LAGRRRRRRRRRK, containing nine arginines, was manually prepared on a peptide-synthesis column by solid-phase peptide-synthesis method. Synthesis was on Rink resin (Novabiochem, USA) using 9-fluorenylmethyloxycarbonyl (Fmoc)-protected amino acids with standard benzotriazole-1-yl-oxy-tris-(dimethylamino)-phosphonium hexafluorophosphate/*N*-hydroxybenzotriazole coupling chemistry. All amino acids use standard side-chain protecting groups, except lysine reside which contained a (4,4-dimethyl-2,6-dioxocyclohex-1-ylidene)ethyl (Dde) functionality protecting the ε-amino group of lysine to allow orthogonal synthesis by selective deprotection of the Dde when the peptide was attached to the resin.

Synthesis of Gd-DTPA-CPPs. After completion of the synthesis and final selective deprotection of the Dde, diethylenetriaminepentaacetic acid anhydride (DTPA, purity 95%, Sigma–Aldrich) was added to react with the ε-amino group of lysine of cell-penetrating peptides resin by dissolving 0.05 mol DTPA in 1 ml of dimethyl sulfoxide (DMSO) and 4 ml of dimethylformamide (DMF) and reacting the DTPA solution with the 0.05 mol peptide resin, which had been washed previously with *N*,*N*′-diisopropylethylamine and dichloromethane. The coupling of DTPA was allowed to proceed with stirring overnight at RT. Completion of the reaction was verified by a negative ninhydrin reaction. DMF was removed, and resin was washed twice each with DMF followed by acetonitrile and then dried under nitrogen. The peptide was cleaved from resin, and the protecting groups were removed by stirring in trifluoroacetic acid (TFA) stock solution [(TFA (10 ml), phenol (0.75 g), thioanisole (0.5 ml), deionized water (0.5 ml), and ethanedithiol (0.25 ml)) at room temperature for 3 h. The cleaved and deprotected peptide was then filtered through glass wool to separate from the resin, precipitated in cold mixture of ether and ethanol (V/V = 1:1), pelleted by centrifugation, and the supernatant removed. Finally, pelleted peptide was dissolved in deionized water and reacted with gadolinium (III) oxide (Gd_2O_3 Sinopharm Chemical Reagent Co, Ltd, Shan hai, China) overnight at 37 °C and precipitated in cold mixture of ether and ethanol (V/V = 1:1), pelleted by centrifugation, and lyophilized to obtain dried crude product. Purification was carried out by C18 column (BONDAPAKTM C18 P/N84176 5 μm Water, USA) on liquid chromatography (BioCAD 700E Perfusion Chromatography Work Station, USA) and identified by Voyager MALDI-TOF mass spectrometry (Applied Biosystems, USA). The white peptide was stored in −20 °C.

Synthesis of FITC-CPPs. The method was same as the above described. Fluorescein-5-isothiocyanate (FITC) was added in 30 mg of peptide resin suspended in 30–35 μl of anhydrous triethylamine. N-terminal coupling was allowed to proceed with stirring for 5 h. DMF was removed, and resin was washed twice each with DMF followed by acetonitrile and then dried under argon. The peptide was cleaved from resin, and the protecting groups were removed by stirring in TFA stock solution [(TFA (10 ml), phenol (0.75 g), thioanisole (0.5 ml), deionized water (0.5 ml), and ethanedithiol (0.25 ml)) at RT for 3 h. The cleaved and deprotected peptide was then filtered through glass wool to separate from the resin, precipitated in cold mixture of ether and ethanol (V/V = 1:1), pelleted by centrifugation, and lyophilized to obtain dried crude product. Purification was carried out by chromatography and identified by MALDI-TOF MS. The light yellow peptide was stored in −20 °C.

Magnetic resonance relaxivity measurement. T1 data for relaxivity determinations were obtained at 17 °C in a VIRIVAN INVOA 400 MHz nuclear magnetic spectroscopy equipped with high-performance gradient coils (100 μs rise time). Gd-DTPA-CPPs and diethylenetriaminepentaacetic acid gadolinium (Gd-DTPA Schering) were prepared in deionized water to be of different concentration and individual T1 values were estimated using a standard inversion recovery pulse sequence with 25–30 delay times. The relaxivity was determined by fitting 1/T1 versus contrast agent concentration using standard linear regression methods [6].

Isolation and expansion of bone marrow mesenchymal stem cells (MSCs). Baby male Sprague–Dawley rats (one week, 10–15 g) were purchased from Animal Administration Center of Xi'an Jiao Tong University. All animal experimental protocols were approved by the Animal Care and Use Committee of University. MSCs were isolated and harvested as previously described [7]. In brief, bone marrow was collected from the femur of the rats. Bone-marrow mononuclear cells were isolated through Percoll (1.073 g/ml) gradient centrifugation (900*g* 3 min) and resuspended in the Dulbecco's modified Eagle's media-low glucose (DMEM, Life Technologies) supplemented with 15% FBS (Hyclone-Pierce, USA) and plated on plastic flasks. Cells were incubated in 95% air and 5% CO_2 at 37 °C and media were replaced first at 48 h. And then every 48 h, the adherent cells were washed twice consecutively in D-Hanks' balanced salt solution. At 80% confluence, cells were harvested with 0.25% trypsin and passaged at a ratio of 1:3. The medium was changed twice a week, by which almost all the hematopoietic stem cells were washed away. To identify MSCs, osteogenic differentiations were performed. MSCs were divided into two groups and, respectively, cultured in the osteogenic medium or control medium. After incubation for three to four days, cells were stained by modified Gomori and von Kossa, as described [8,9].

CPPs uptake assays. Labeling with fluorescein was to identify the penetration and location of CPPs in MSCs. Just before the study, FITC-CPPs and FITC were freshly diluted in DMEM to obtain 25 nmol/ml solutions. MSCs (3×10^6 per group) were, respectively, stained with 25 nmol/ml FITC-CPPs for 10 min and FITC for 60 min in RT. Cells were washed by D-Hanks' balanced salt solution without fixation. Then live cells were imaged on inverted fluorescence microscope (OLYMPUS IX50, Japan) and analyzed by flow cytometry at 520-nm emission for FITC-labeled cells.

MR imaging in vitro. Just before the study, Gd-DTPA-CPPs and Gd-DTPA were freshly diluted in DMEM with 15% FBS to obtain solutions in the concentration of 0, 30, 60, 90, and 120 nmol/ml. In the first experiment, MSCs (3×10^6 per group) were, respectively, incubated with the above solution for 60 min. In the second experiment, MSCs (3×10^6 per group) were, respectively, incubated with 60 nmol/ml for 0, 10, 30, 60, 90, and 120 min. After incubating in the above-mentioned steps, the solution was abandoned and cells were washed by D-Hanks' solution (HBSS) five times, trypsinized for 2 min, then cells were centrifuged, then the cell pellet was suspended in 400 μl of 1.0% agarose in HBSS in a 500 μl Eppendorf tube. The Eppendorf tubes were placed in a beaker containing the above 1.0% agarose solution and imaged with the 1.5 T-superconducting magnet (SIGNA EXCITE 1.5 T GE) using a 3-inch surface coil. The imaging protocol consisted of transverse T1 weighted fast spin-echo (TR 440 ms,TE 13 ms, FOV 12 mm, slice thickness 2 mm, gap 0.2 mm, matrix 288 × 192, NSA4, flip angle 90°), Then the T1 signal intensities in tube (Iin) and of agarose (Iout) were measured. Triplicate measurements were averaged to obtain each data point.

Cytotoxicity assay. To determine whether Gd-DTPA-CPPs would be more toxic to normal cell, MSCs (1×10^3 cells/well) were seeded in a 96-well cell culture plate and incubated with the above-mentioned five concentrations and the control culture media for a period of 72 h. Four hours before the end of the incubation, 20 μl of MTT solution was added into each well containing cells and the plate incubate in a CO_2 incubator at 37 °C for 4 h. Media were removed and 200 μ1 of DMSO was added to each well and pipette up and down to dissolve crystals. The plate was placed into the 37 °C incubator for 5 min. It was then transfered to plate reader (BMG Labtechnologies, USA) and absorbance was measured at 550 nm.

Flow cytometric analysis. After cells were incubated with the above-mentioned five concentrations for 72 h, the extent of apoptosis was determined using the annexin-V-FITC kit (DingGuo Bio, Peking). Briefly, the treated cells were first stained with annexin-V-FITC in the presence of calcium 1.5 mM for 10 min at 0 °C, according to the manufacturer's protocol. The adherent cells were then harvested by trypsinization and combined with detached cells. Total cells were stained with 2.5 mg/ml propidium iodide (PI) for 15 min on ice and analyzed immediately by flow cytometry (TCX-NT, Leica). Apoptotic cells were gated based on low propidium iodide and high annexin-V staining. Readings were taken at

490 nm excitation and 520 emission (PI: 530 nm excitation, 617 nm emission) wavelengths with 10,000 cells counted per sample. The values were reported as percentages of total cells counted. The other experiment was for evaluating the damage of mitochondria from new imaging media with specific fluorescent probe, Rhodamine123 (Rh123). Briefly, after the treated cells were stained with 10 μg/ml Rh123 (Sigma) for 20 min at 37 °C, the washed cells were collected and analyzed at 503 nm excitation and 527 emission immediately by flow cytometry.

Images and statistical analysis. Visualization analysis and half-quantitative analysis were used for determining the signal characteristics and the statistical significance of differences among each group. The T1WI signal intensity of 5 groups (I in) and the intensity of 1% agarose (I out) were acquired by region of interest (ROI). By SPSS13.0, the ANOVA was performed to compare the signal difference among groups and the toxicity of Gd-DTPA-CPPs to MSCs. Group differences among groups were considered to be significant if $p < 0.05$.

Table 1
Determination of relaxivity of CPPs-DTPA-Gd in water

Agents	Concentration (mmol/l)	T1 (s)	R ($M\ m^{-1}\ s^{-1}$)
Gd-DTPA	0.5	0.0522 ± 0.0101	4.4926 ± 0.0078
	0.25	0.0558 ± 0.0016	
	0.125	0.0578 ± 0.0003	
CPPs -DTPA-Gd	0.5	0.05113 ± 0.0002	5.7311 ± 0.0122*
	0.25	0.05430 ± 0.0010	
	0.125	0.05791 ± 0.0009	

Relaxivity is measured on 400 MHz NMR at 17 °C.
* Compared with Gd-DTPA, T1 relaxivity of CPPs-DTPA-Gd increased significantly (paired t test $t = -1659.566$, $p < 0.001$).

Results

Purification of crude peptide was accomplished by using reversed phase C-18 column at reversed-phase high-pressure liquid chromatography (HPLC) at a flow rate of 4 ml/min by an eluent mixture of 0.1% TFA in 5% acetonitrile/95% water and 0.1% TFA in 90% acetonitrile/10% water. The main fraction (Gd-DTPA-CPPs retention time = 14.41 min, FITC-CPPs retention time = 14.19 min) was collected and found to be Gd-DTPA-CPPs and FITC -CPPs by TOF-MS (Gd-DTPA-CPPs $m/z = 2285.99$, calcd value = 2285.78. FITC-CPPs $m/z = 2163.34$, calcd value = 2163.55). Relaxivity was determined by spin-lattice relaxation time (T1) and concentration. The dependence of 1/T1 on contrast agent concentrations for Gd-DTPA-CPPs and Gd-DTPA in water was demonstrated in Table 1, T1 relaxivity of Gd-DTPA-CPPs was (5.7311 ± 0.0122) $Mm^{-1}\ s^{-1}$, significantly higher than that of Gd-DTPA. ($t = 1659.566$, $p < 0.001$).

After continued to refresh culture media in 3 days, two cell phenotypes of attached marrow stromal cells were observed (Fig. 1A): large spindle-shaped cells and lesser populations of smaller round cells. This result was similar to observations reported in the literature of a mixed population of mesenchymal progenitor cells from human bone marrow stroma [10]. After 7 days of cultures, the attached cells significantly increased to 90% confluence and the cells were noted to have a large expansive potential. When incubated in medium supplemented with dexamethasome,

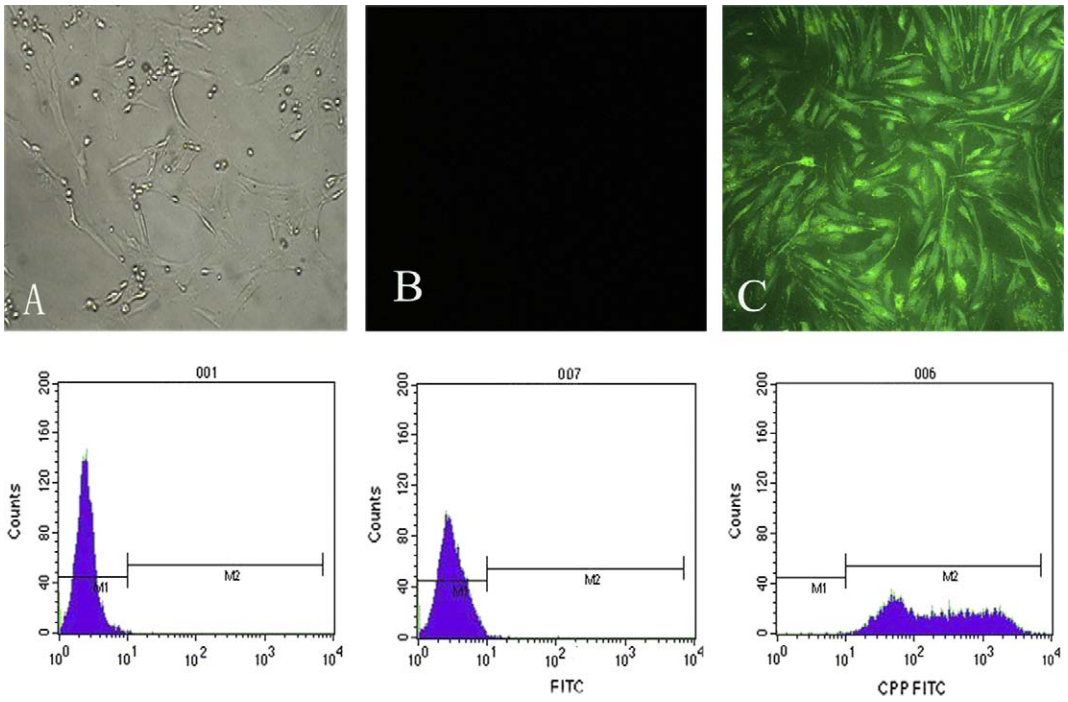

Fig. 1. Translocation of FITC into MSCs depends on CPPs, as demonstrated by microscopy (A–C) and FACS analysis (001, 007, and 006): (A) by microscopy shows the confluent growth of primary MSCs cultured for 9 days after seeding 40×. (B) By inverted fluorescence microscopy shows no fluorescence in MSCs incubated only with FITC. (C) By inverted fluorescence microscopy shows significant fluorescence in MSCs incubated with FITC-CPPs. FACS analysis: 001 shows the untreated cells. 007 and 006, respectively, show cells incubated with FITC and FITC-CPPs.

β-glycerophosphate and ascorbic acid-2-phosphate, the MSCs underwent differentiation into osteoblasts, showing positive stain of alkaline phosphatase activity and the black precipitation of calcium salts (Fig. 2).

Cellular uptake was half-quantitated by using FITC-labeled CPPs and by using gadolinium-DTPA-CPPs conjugate on MRI T1 weighted imaging (TIWI) signal intensity. FITC labeled with CPPs was used directly to determine the ability of penetration and subcellular localization of CPPs. Fluorescence can be observed in cytoplasm and nucleus of MSCs incubated with CPPs-FITC (Fig. 1B and 1-007) for 10 min at 37 °C and no fluorescein was observed in MSCs incubated with FITC (Fig. 1C and 1-006). Gd-DTPA-CPPs translocated into MSCs were detected by MR imaging in vitro. Compared with the control group, the groups incubated with Gd-DTPA-CPPs had a increasingly high T1 signal and the T1 signal of groups incubated with Gd-DTPA was similar to the control group (Fig. 3). By region of interest (ROI), the T1 signal increased with the incubating time (Table 2) and concentrations in the groups incubated with Gd-DTPA-CPPs (Table 3). This result suggested that the CPPs was required for translocation of gadolinium, and the capability of internalization was similar to Tat peptides as reported [30]. Cytotoxicity assay was used to determine whether Gd-DTPA-CPPs analogues would be toxic to MSCs by MTT and Flow cytometric analysis. In Table 4, the effect of Gd-DTPA-CPPs on cell viability was compared with the control cells. After incubation for 72 h, MTT show all cell groups had similar responses to the new imaging agents even in a concentration of 120 nmol/ml, suggesting having less effect on viability in tested concentrations. Cells that are in earlier stages of apoptosis can be stained with annexin-V but they exclude PI. However, cells in late stages of apoptosis or necrosis cannot exclude PI due to damaged cellular membrane. Based on this principle, cytotoxicity can be evaluated with annexin-V/PI double staining Fig. 4. Four concentrations' treatment was found to have no significant effect, compared with the control cells, as shown in Table 5. Functional mitochondria displaying (Fig. 5) a normal membrane potential gradient were identified with rhodamine 123 (Rh123), four used concentrations were found to have no significant effect on mitochondria membrane potential gradient, compared with the control cell group.

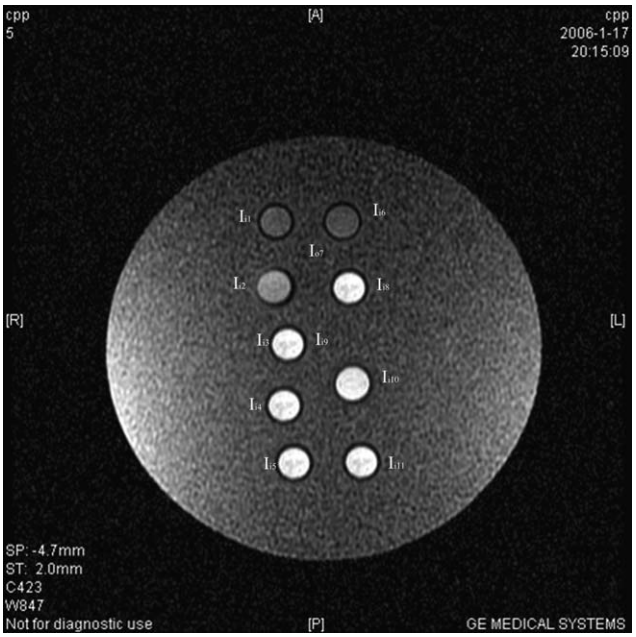

Fig. 3. A value of 1.5 T MR T1WI signal of MSCs incubated with contrast medium: (R) I_{i1} represents the T1 signal of the control group, I_{i2}, I_{i3}, I_{i4}, and I_{i5}, respectively, represent the T1 signal of the groups 2, 3, 4, and 5. (L) I_{i6} represents the T1 signal of the group 6 (cell incubated with 120 nmol/ml Gd-DTPA for 60 min); I_{i8}, I_{i9}, I_{i10}, and I_{i11}, respectively, represents the T1 signal of the groups 8, 9, 10, and 11; I_{i7} represents the T1 signal of the background (group 7).

Discussion

The bone marrow stroma contains a subset of nonhematopoietic cells referred to as mesenchymal stem or mesenchymal progenitor cells (MSCs). These cells have the capacity [10] to undergo extensive replication in an undifferentiated state ex vivo. In addition, MSCs have the potential to develop either in vitro or in vivo into distinct mesenchymal tissues, including bone, cartilage, fat, tendon, muscle, and marrow stroma, which suggests these cells as an attractive cell source for tissue engineering approaches.At the same time, the ability of MSCs to migrate is

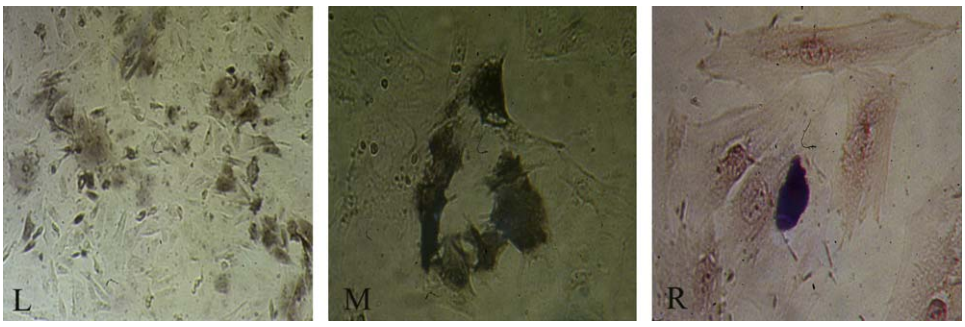

Fig. 2. Osteogenic differentiation of MSCs (L, positive expression of ALP cytochemical staining in 4-day induction 40×; M, positive expression of ALP cytochem ical staining in a-week induction 100×; R, weak-positive expression of calcium salts by von Kossa staining after a week induction 100×).

Table 2
Relationship between T1WI signal intensity and incubating time

ROI	Cell incubated in CPPs -DTPA- Gd				Cell incubated with Gd-DTPA (I_{i6})	Control group (I_{i1})	Background (I_{o7})
	10 min (I_{i2})	30 min (I_{i3})	60 min (I_{i4})	90 min (I_{i5})			
Tube 1	1271.58	1996.79	2469.93	3012.99	754.31	753.57	571.14
Tube 2	1289.75	1879.57	2304.51	3144.68	762.12	772.01	557.32
Tube 3	1237.36	1884.94	2673.4	3085.93	759.33	758.49	603.65
M ± S	$1266.23 \pm 26.60^{\Delta\Delta}$	$1920.43 \pm 66.18^{@}$	$2482.61 \pm 184.77^{**}$	$3081.20 \pm 65.97^{\#\#}$	$758.59 \pm 3.96^{\Delta}$	$761.36^{*,\#} \pm 9.55$	577.37 ± 23.79

All groups of MSCs were incubated with contrast medium in a concentration of 60 nmol/ml. ANOVA of seven groups: $F = 2911.08$, $p < 0.001$. LSD-t between each two groups: *group 1 and group 6, $p = 0.948$, $^{\#}$group 1 and groups 2, 3, 4, 5, 7, $p < 0.001$, $^{\Delta\Delta}$group 2 and groups 3, 4, 5, 6, 7, $p < 0.001$. $^{@}$Group 3 and groups 4, 5, 6, 7, $p < 0.001$, **group 4 and groups 5, 6, 7, $p < 0.001$, $^{\#\#}$group 5 and groups 6, 7, $p < 0.001$, $^{\Delta}$group 6 and groups 2, 3, 4, 5, 7, $p < 0.001$, relation among group 1 to group 5: $r = 0.993$ ($p < 0.001$).

Table 3
Relationship between T1WI signal intensity and incubating concentration

ROI	Cell incubated in Gd-DTPA-CPP				Cell incubated with Gd-DTPA (I_{i6})	Control cell (I_{i1})	Background (I_{o7})
	30 nmol/ml (I_{i8})	60 nmol/ml (I_{i9})	90 nmol/ml (I_{i10})	120 nmol/ml (I_{i11})			
Tube 1	2011.37	2469.93	3127.65	3871.03	754.31	753.57	571.14
Tube 2	1974.26	2304.51	2998.71	4001.21	762.12	772.01	557.32
Tube 3	1999.29	2673.40	3088.44	3884.26	759.33	758.49	603.65
M ± S	$1994.97 \pm 15.69^{\&}$	$2482.61 \pm 153.01^{@}$	$3071.60 \pm 54.68^{**}$	$3918.83 \pm 59.21^{\#\#}$	758.59 ± 3.96	$761.36 \pm 9.55^{*,\Delta}$	$577.37 \pm 23.79^{\Delta\Delta}$

All groups of cells were incubated with contrast medium for 60 min. ANOVA of seven groups: $F = 15394.71$; $p < 0.001$. LSD-t between each two groups: *group1and group 6, $p = 0.948$, $^{\Delta}$group 1 and groups 7, 8, 9, 10, 11, $p < 0.001$, $^{\&}$group 8 and other six groups $p < 0.001$, $^{@}$group 9 and groups 10, 11, 6, 1, 7, $p < 0.001$, **group10 and groups 11, 6, 1, 7, $p < 0.001$, $^{\#\#}$group 11 and groups 1, 6, 7, $^{\Delta\Delta}$group 7 and other six groups $p < 0.001$, relation among group 1 and groups 8, 9, 10, 11: r=0.986 ($p < 0.001$).

Table 4
Cytotoxicity of Gd -DTPA- CPP for MSCs (MTT)

A550	Concentration				
	0 nmol/ml	30 nmol/ml	60 nmol/ml	90 nmol/ml	120 nmol/ml
No.1	1.1998	1.2011	1.1886	1.1976	1.1991
No.2	1.2003	1.1898	1.1907	1.2010	1.8766
No.3	1.1964	1.2100	1.2064	1.1945	1.2105
No.4	1.1990	1.1904	1.1973	1.1989	1.1913
M ± S	1.1989 ± 0.0017	1.1978 ± 0.0096	1.1958 ± 0.0080	1.1980 ± 0.0027	1.1994 ± 0.3382

All groups of cells were incubated with contrast medium for 72 h. ANOVA of five groups: $F = 1.030$; $p = 0.424$.

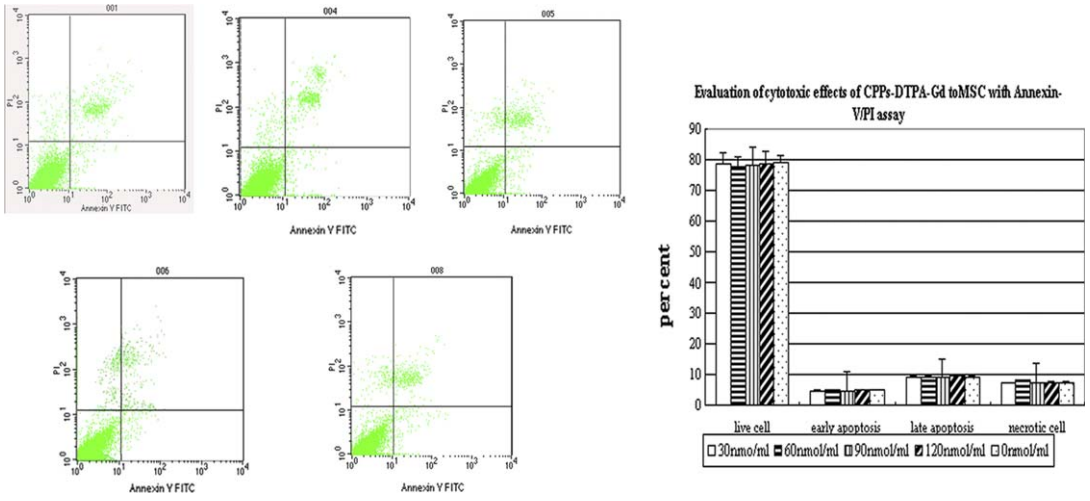

Fig. 4. Apoptosis analysis by FITC-annexin-V/PI flow cytometry: 001 shows the control MSCs (incubated with 0 nmol/ml), 004, 005,006, and 008, respectively, represent the MSCs incubated with Gd-DTPA-CPPs in the concentration of 30, 60, 90, and 120 nmol/ml. The column artwork shows apoptosis difference among five groups.

Table 5
Evaluation of cytotoxic effects of CPPs-DTPA-Gd to MSCs with Annexin-V/PI assay

Exposure annexin-V/PI stain	Live cells (%)	Early apoptotic cells (%)	Late apoptotic cells (%)	Necrotic cells (%)
30 nmol/ml	78.54 ± 0.61	4.60 ± 0.26	9.11 ± 0.06	7.08 ± 0.71
60 nmol/ml	77.01 ± 1.30	4.78 ± 0.17	9.18 ± 0.21	7.79 ± 0.85
90 nmol/ml	77.55 ± 1.50	4.71 ± 0.42	9.01 ± 1.24	7.49 ± 0.84
120 nmol/ml	78.70 ± 0.75	4.85 ± 0.07	9.38 ± 0.05	7.33 ± 0.10
0 nmol/ml (control)	78.51 ± 0.53	4.89 ± 0.15	9.25 ± 0.26	7.35 ± 0.53

The percent of live, early and late apoptotic or necrotic cells following treatment with CPPs-DTPA-Gd. As assessed by the annexin-V and PI staining assay. Data shown are means ± SE, percentage of staining. The percent of cells stained as annexin-V-/PI-(live), annexin-V+/PI-(early apoptotic), annexinV+/PI+(late apoptotic), and annexinV-/PI+(necrotic cells) is presented. ANOVA of cell apoptosis in five concentrations: live cell $F = 0.442$, $p = 0.776$; early apoptotic cell $F = 1.647$, $p = 0.238$; late apoptotic cell $F = 0.580$, $p = 0.684$; necrotic cell $F = 1.122$, $p = 0.399$.

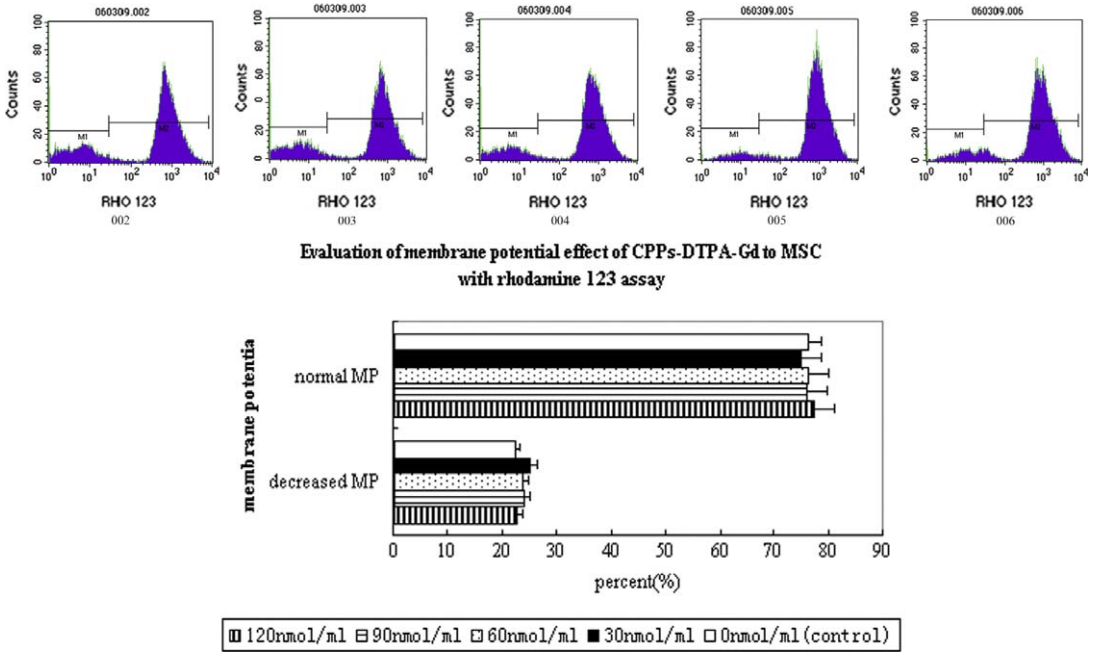

Fig. 5. MSCs membrane potential (MP) gradient analysis by rhodamine 123 flow cytometry: 002 shows the control MSCs (incubated with 0 nmol/ml), 003, 004, 005, and 006, respectively, represent the MSCs incubated with Gd-DTPA-CPPs in the concentration of 30, 60, 90, and 120 nmol/ml. The column artwork shows the change of membrane potential gradient difference among five groups.

critical during developmental events in embryogenesis, in the function of mature cells, in vascular remodeling during angiogenesis, and in most immune and infectious diseases. Huge advances in understanding these events can potentially be gained by investigating cell migration in vivo. Several methods [11,12] are described for isolated MSCs. In this research, mesenchymal stem cells were separated by gradient density centrifugation and adherence. Expression of alkaline phosphatase (AP) is a marker of cells capable of differentiation into osteoblasts. Experimental analysis of differentiation potential of mesenchymal precursors widely uses this enzyme as a marker of osteogenic cells. Here we used the modified Gomori assay for alkaline phosphatase as a marker of MSCS of rat bone marrow. After four days' induction in the osteogenic medium including dexamethasone, β-glycerophosphate, and ascorbic acid-2-phosphate [13], most cells in the colonies derived from the rat bone marrow were weakly AP-positive, which suggests the osteogenic potential of MSCs.

Because of the importance of MSCs, now, the goal of noninvasive imaging of stem cell migration, and specifically of genetically engineered stem cells, has long been sought. Traditionally, cells have been followed by technically challenging and invasive chamber models using intravital microscopy [14,15] or by using flow cytometry analysis of fluorescently labeled cells recovered from excised tissues [16,17]. Recent developments in MR imaging have enabled in vivo imaging at near microscopic resolution [18,19]. In order to visualize and track stem cells by MR imaging, it is necessary to tag cells magnetically. Conventional magnetic cell labeling techniques rely on surface attachment of magnetic beads [20] ranging in size from several hundred nanometers to micrometers. Although these methods are efficient for in vitro cell separation, cell surface labeling is

generally not suitable for in vivo use because of the rapid reticuloendothelial recognition and clearance of cells thus labeled. Alternatively, lymphocytes and other cells have been labeled with small monocrystalline nanoparticles ranging in sizes from 10 to 40 nm using fluid-phase or receptor-mediated endocytosis. Unfortunately, the labeling efficiency is generally low. During the last decade, several proteins and peptides have been found to traverse through the cellular membranes in a process called "protein transduction", delivering their cargo molecules into the cytoplasm and/or nucleus. These proteins and peptides have been used for intracellular delivery of various cargoes with molecular weights several times greater than their own. This process of protein transduction was discovered first by Green [21] and Frankel [22] independently, who found that 86-mer *trans*-activating transcriptional activator (TAT) from HIV-1 was efficiently taken up by various cells, when added to the surrounding media. Subsequently, this property of translocation was found in a series of short peptides [23–28]. More precisely, their ability to translocate across the plasma membranes is confined to short sequences of less than 20 amino acids, which are highly rich in basic residues. Such sequences are called cell-penetrating peptides (CPPs) or membrane permeable peptide (MPP) or protein transduction domain (PTD). According to a recently suggested classification [29], CPPs can be arranged in three classes: (I) protein-derived CPPs such as TAT, penetratin. (II) Model peptides such as MAP, arginine$_{(6,7,9)}$. (III) Designed CPPs such as MPG, transportan. Although mechanism of internalization of CPP has not been resolved completely [29], it has been observed that many molecules carried by CPPs can be translocated into the cell, including protein, antibody, DNA, liposomes, nanoparticles, etc., which supplied a new way to molecular imaging. B. Rajeev et al. [30] demonstrated that HIV-TAT$_{(48–58)}$ can translocate ^{111}In-DOTA and Gd-DOTA into fresh lymphocytes and the uptake increases with incubating time and concentration. Andrew et al. [6] showed TAT-DOTA-Gd can cross the cell membrane into lymphocytes and the relaxivity is better than Gd-DTPA. Those researches suggest CPPs could translocate imaging agents into MSCs for tracking. B. Fabienne et al. [31] suggest that arginine(9) can more effectively transport than TAT and penetratin, so in this research, an arginine(9)-based CPP is used to label gadolinium and fluorescein-5-isothiocyanate for two aims, one is to determine whether the newly constructed short peptide still has the ability to translocate imaging agents into the cell and the other aim is to observe whether MSCs labeling with the new peptide carrying Gd-DTPA can be detected by MRI. After MSCs are incubated with FITC-CPPs, fluorescence can be observed in cytoplasm and nucleus of MSCS incubated with FITC-CPPs, but no fluorescein was observed in MSCS incubated with FITC, which suggest the newly constructed peptide effectively transports the cargo. Gd-DTPA is a kind of MRI contrast agent which distributes in extracellular spaces in this experiment. Compared with Gd-DTPA, the relaxivity of gadolinium labeled with CPPs (Gd-DTPA-CPPs) in water determined by 400 MHz NMR is increased, which suggests this new agent could shorten T1 and increase T1WI contrast signal. MR imaging in vitro shows MSCS labeling with the new peptide via Gd-DTPA has a higher T1WI signal detected by MRI and the T1WI signal increases in a concentration- and time-dependent model without reaching saturation in the detected concentrations and incubation time. These suggest CPPs are required for Gd-DTPA translocation and can be used for MSCS tracking. MTT assay to determine whether Gd-DTPA-CPPs would be toxic to MSCS suggests, compared with the control groups, no more toxicity from Gd-DTPA-CPPs. Apoptosis further analyzed by FITC-annexin-V/PI flow cytometry shows new intercellular imaging agents do not obviously lead to apoptosis. Functional mitochondria displaying a normal membrane potential gradient were identified with rhodamine 123 (Rh123), a cationic fluorescent probe. The gradient allows the transport of the probe across the outer membrane to the inner one where it remains because of charge interactions. Four concentrations' treatment was found to have no significant effect on mitochondria membrane potential gradient, compared with the control cell group by Rh123 assay, which suggested that Gd-DTPA-CPPs in the tested concentration should not effect the function of mitochondria.

The intracellular delivery of compounds designed to interact with specific intracellular targets by attachment to cell penetrating peptides could have far-reaching implications for both in vitro and in vivo applications of molecular imaging. Furthermore, MSCs tracking in vivo by CPPs needs to be done.

Acknowledgments

The authors acknowledge the valuable help of Dr. Lingyu Zhao and Qin Li for assisting ALP stain, Dr. Ning Du in assiting von Kossa stain, Dr. Shen Nian for assisting MTT assay, Professor Jun-jie Zhao for assisting peptides purification, Dr. Dian-zen Zhang for assisting flow cytometric analysis, Dr. Min Xu and Yi-li Zhang in assisting cell MR imaging experiments, and Professor Ren-hua Wu for many fruitful discussions and review of the manuscript. This work was supported by the Doctoral Foundation of Xi'An Jiao Tong University (dfxjtu2005-09).

References

[1] Robert J. Deans, Annemarie B. Moseley, Mesenchymal stem cells: biology and potential clinical uses, Exp. Hematol. 28 (2000) 875–884.
[2] M.D. Steven, M.B. Amelia, M. Nadim, N. Mary, P. Sheila, H. Wayne, S. Cord, H. Terry, C. Theodore, S. Wendy, S. Dorie, W. Scott, F. Karen, M. Joseph, D. Robert, M. Annemarie, H. Ronald, Mesenchymal stem cells are capable of homing to the bone marrow of non-human primates following systemic infusion, Exp. Hematol. 29 (2001) 244–255.
[3] Jun Ma, Junbo Ge, Shaoheng Zhang, Aijun Sun, Jianying Shen, Leilei Chen, Keqiang Wang Yunzeng Zou, Time course of myocardial

stromal cell-derived factor 1 expression and beneficial effects of intravenously administered bone marrow stem cells in rats with experimental myocardial infarction, Basic Res. Cardiol. 100 (2005) 1–7.
[4] Jochen Ringe, Christian Kaps, Gerd-Rüdiger Burmester, Michael Sittinger, Stem cells for regenerative medicine: advances in the engineering of tissues and organs, Naturwissenschaften 89 (2002) 338–351.
[5] B. Gupta, T.S. Levchenko, V.P. Torchilin, Intracellular delivery of large molecules and small particles by cell-penetrating proteins and peptides, Adv. Drug Deliv. Rev. 57 (2005) 637–651.
[6] M.P. Andrew, S. Vijay, R.G. Joel, P.W. David, Synthesis and characterization of a Gd-DOTA-D-Permeation peptide for magnetic resonance relaxation enhancement of intracellular targets, Mol. Imaging 2 (2003) 333–341.
[7] Xin-Qin Kang, Wei-Jin Zang, XiaoLi Xu, Tu-Sheng Song, Xiao-Kiang Yu, Ju-Rong Zeng, Differentiation characteristics of rat mesenchymal stem cells in vitro, J. Fourth Mil. Med. Univ. 25 (2004) 1252–1255.
[8] Zhe Zhang, Hui Chen, Cheng-ku Li, The methods of alkaline phosphatase staining, in: Zhe Zhang, Hui Chen (Eds.), The Manual of Pathological Staining Technique, Liao Ning, 1988, pp. 254–255.
[9] Zhe Zhang, Hui Chen, Cheng-ku Li, The methods of calcium staining, in: Zhe Zhang, Hui Chen (Eds.), The manual of pathological staining technique, Liao Ning, 1988, pp. 177–178.
[10] D.J. Prockop, I. Sekiya, D.C. Colter, Isolation and characterization of rapidly self-renewing stem cells from cultures of human marrow stromal cells, Cytotherapy 3 (2001) 393–396.
[11] S.C. Hung, N.J. Chen, S.L. Hsieh, H. Li, H.L. Ma, W.H. Lo, Isolation and characterization of size sieved stem cells from human bone marrow, J. Stem Cells 20 (2002) 249–258.
[12] T. Soukup, J. Mokry, J. Karbanova, R. Pytlik, P. Suchomel, L. Kucerova, Mesenchymal stem cells isolated from the human bone marrow: cultivation, phenotypic analysis and changes in proliferation kinetics, Acta Medica (Hradec Kralove) 49 (2006) 27–33.
[13] Xinqin Kang, Weijin Zang, Xiaoli Xu, Tusheng Song, Xiaojiang Yu, Jurong Zeng, Change of ALPase during the differentiation into osteoblast from rat marrow mesenchymal stem cells, J. Xipan Jiaotong University (Medical Sciences) 25 (2004) 366–368.
[14] U.H. von Andrian, C. M'Rini, In situ analysis of lymphocyte migration to lymphnodes, Cell Adhes. Commun. 6 (1998) 85–96.
[15] M.D. Menger, H.A. Lehr, Scope and perspectives of intravital microscopy bridge over from in vitro to in vivo, Immunol. Today 14 (1993) 519–522.
[16] P.J. Hendrikx, A.C.M. Martens, A. Hagenbeek, J.F. Heij, J.W.M. Visser, Homing of fluorescently labeled murine hematopoietic stem cells, Exp. Hematol. 24 (1996) 129–140.
[17] S.M. Lanzkron, M.I. Collector, S.J. Sharkis, Hematopoietic stem cell tracking in vivo: a comparison of short-term and long-term repopulating cells, Blood 93 (1999) 1916–1921.
[18] S. Choi, X. Tang, D. Cory, Constant time imaging approaches to NMR microscopy, Int. J. Imaging Sci. Technol. 8 (1997) 263–276.
[19] R.E. Jacobs, E.T. Ahrens, T.J. Meade, S.E. Fraser, Looking deeper into vertebrate development, Trends Cell Biol. 9 (1999) 73–76.
[20] R. Weissleder, H. Cheng, A. Bogdanova, A.J. Bogdanov, Magnetically labeled cells can be detected by MR imaging, J. Magn. Reson. Imaging 7 (1997) 258–263.
[21] M. Green, P.M. Loewenstein, Autonomous functional domains of chemically synthesized human immunodeficency virus TAT *trans*-activator protein, Cell 55 (1988) 1179–1188.
[22] A.D. Frankel, C.D. Pabo, Cellular uptake of the TAT protein from human immunodeficency virus, Cell 55 (1988) 1189–1193.
[23] Joliot, C. Pernelle, H. Deagostini-Bazin, A. Prochiantz, Antennapedia homeobox peptide regulates neural morphogenesis, Proc. Natl. Acad. Sci. USA 88 (1991) 1864–1868.
[24] G. Elliott, P. O'Hare, Intercellular trafficking and protein delivery by a herpesvirus structural protein, Cell 88 (1997) 223–233.
[25] M. Pooga, M. Hallbrink, M. Zorko, U. Langel, Cell penetration by transportan, FASEB J. 12 (1998) 67–77.
[26] Shigeyuki Namiki, Taichiro Tomida, Mao Tanabe, Masamitsu Iino, Kenzo Hirose, Intracellular delivery of glutathione *S*-transferase into mammalian cells, Biochem. Biophys. Res. Commun. 305 (2003) 592–597.
[27] J.B. Rothbard, S. Garlington, Q. Lin, T. Kirschberg, E. Kreider, P.L. McGrane, P.A. Wender, P.A. Khavari, Conjugation of arginine oligomers to cyclosporin A facilitates topical delivery and inhibition of inflammation, Nat. Med. 6 (2000) 1253–1257.
[28] Hirofumi Noguchi, Masayuki Matsushita, Shinichi Matsumoto, Yun-Fei Lu, Hideki Matsui, Susan Bonner-Weir, Mechanism of PDX-1 protein transduction, Biochem. Biophys. Res. Commun. 332 (2005) 68–74.
[29] Matjaz Zorkoa, Ulo Langel, Cell-penetrating peptides: mechanism and kinetics of cargo delivery, Adv. Drug Deliv. Rev. 57 (2005) 529–545.
[30] Rajeev Bhorade, Ralph Weissleder, Tsunenori Nakakoshi, Anna Moore, Ching-Hsuan Tung, Macrocyclic chelators with paramagnetic cations are internalized into mammalian cells via a HIV-tat derived membrane translocation peptide, Bioconjugate Chem. 11 (2000) 301–305.
[31] B. Fabienne, S. Sagan, G. Bolbach, G. Chassaing, Quantification of the cellular uptake of cell-penetrating peptides by MALDI-TOF mass spectrometry, Angew Chem. Int. Ed. 44 (2005) 4244–4247.